Scale dependence in functional equivalence and difference in the soil microbiome

Alexander Polussa[1]* (ORCID: 0000-0002-5559-9984), Javier Gonzalez-Rivero[1], Nicholas Fields[1], Fiona V. Jevon[1] (0000-0002-3586-7566), Stephen A. Wood[1,2] (0000-0002-9551-8165), William R. Wieder[3,4] (0000-0001-7116-1985), and Mark A. Bradford[1] (0000-0002-2022-8331)

[1]*Yale School of the Environment, Yale University, 195 Prospect St., New Haven, CT 06511, USA*

[2]*The Nature Conservancy, Arlington, VA, USA*

[3]*Climate and Global Dynamics Laboratory, National Center for Atmospheric Research, Boulder, CO 80307, USA*

[4] *Institute of Arctic and Alpine Research, University of Colorado, Boulder, CO 80309, USA*

*Corresponding author: alexander.polussa@yale.edu

Abstract

Climatic history can shape the functioning of soil microbial communities and thus rates of ecosystem processes such as organic matter decomposition. For example, broad spatial scale differences in climatic history, such as contrasting precipitation regimes, have been shown to generate unique microbial functional responses to contemporary moisture conditions. Yet it is an open question as to whether local differences in soil microclimate similarly influence the functional potential of decomposer communities. Here, we use a multi-scale approach within and among two temperate forest field sites to investigate this question. Soils from fifty-four microsites, that vary in their soil moisture climate-regimes, were used as inocula for a common leaf litter (*Quercus rubra* L.) in a controlled, laboratory microcosm study. Microcosms were placed under dry, mesic and wet lab-moisture conditions and the rate of carbon (C) mineralization of the litter was measured over 202 days. Our results reveal differences in decomposition rates under controlled conditions that highlight broad-scale functional differences between the soil communities at each site. Specifically, we found that C mineralization differed by as much as two-fold for soil communities when compared between the sites. Our results also show that functional differences of soil communities are observable within one site but not the other. In the site where local-scale functional legacies were apparent, the historical soil moisture microclimate-regimes generated as much as an 89% change in C mineralization rates of the leaf litter under the same contemporary, lab-imposed moisture conditions. A similar pattern was not observable in the other site; instead, laboratory moisture conditions explained almost all variation in C mineralization. Notably, for the site with pronounced local-scale functional legacies, there was much greater within-site variation in field-soil microsite moisture than at the site which did not exhibit functional legacies, suggesting that the extent of local-scale variation

in microclimate may act as control on whether local-scale functional legacies are observed. Regardless of whether this mechanism does explain our findings, our observations do confirm those from prior studies where regional-scale moisture-regime differences shape microbial function, and extend this prior work by providing evidence that pronounced local-scale differences in soil moisture microclimate-regimes are associated with microbial functional legacies.

Keywords

Carbon mineralization, functional redundancy, litter decomposition, legacies, microbial community function, scale, soil moisture, temperate forests

Introduction

Soil heterotrophic microorganisms produce carbon dioxide as they metabolize decomposing organic material for energy and growth (Swift et al., 1979). As biological agents that mediate decomposition, their activities contribute substantially to the fluxes of carbon (C) from terrestrial ecosystems to the atmosphere (Falkowski et al., 2008; Bond-Lamberty and Thomson, 2010). Soil temperature, moisture, and litter quality are important controls on decomposition rates (Aerts, 1997; Parton et al., 2007) and are consequently represented in soil biogeochemical models. These models are used to understand and project how decomposition rates respond to changing environmental conditions, and the inclusion of microbial biomass and community traits as additional controls on organic matter decomposition reflect growing evidence that their influence on decomposition rates extends beyond those mediated directly by abiotic controls (Glassman et al., 2018; Maynard et al., 2018). These modeling efforts have revealed that the way in which microbes are represented can strongly influence projected changes in soil organic matter flux rates and pool sizes (Schimel and Weintraub, 2003; Wang et al., 2013; Wieder et al., 2015b; Abramoff et al., 2018; Fatichi et al., 2019).

There is now a wealth of empirical evidence that the abiotic environment shapes both the structure and function of microbial communities. In experimental manipulations and across environmental gradients, past abiotic regimes of temperature (Karhu et al., 2014; Romero-Olivares et al., 2017), moisture (Evans and Wallenstein, 2012, 2014; Hawkes et al., 2017), and litter input quality (Keiser et al., 2011) have been observed to shape contemporary microbial function (Strickland et al., 2015; Crowther et al., 2019). Additionally, the abiotic historical legacies of these regimes on microbial community function can be persistent. For example, Hawkes et al. (2020) showed that within a regional precipitation gradient, 4.5 years of

70 manipulated rainfall did not significantly shift microbial community function. Instead, soil
71 respiration responses to the rainfall manipulation continued to reflect the community's 'climate
72 origin'. These findings suggest that persistent functional legacies in biotic communities may
73 constrain local ecosystem responses to environmental change, yet it is unclear in which
74 environments and at which scales these legacies manifest (Baveye et al., 2018; Ladau and Eloe-
75 Fadrosh, 2019).

76 Climatic variables are known to vary at both macro- and micro-scales. For instance, soil
77 moisture regimes often vary substantially in space both across and within sites. In forests, spatial
78 variation in soil moisture at local scales (m to km) can be equal in magnitude, or even exceed,
79 variation in site-mean soil moisture among sites arrayed across regional climate gradients
80 (Bradford et al., 2014, 2017; Loescher et al., 2014). Variables including topography, soil
81 properties and plant traits interact to produce microscale heterogeneity in moisture
82 (Vanderlinden et al., 2012), but how microclimatic variation imprints historical legacies on the
83 functioning of microbial communities appears largely unknown. Yet within-site moisture
84 regimes have been linked to patterns in fungal composition and function (van der Wal et al.,
85 2015; Šťursová et al., 2016), enzyme activities (Baldrian et al., 2010, Baldrian, 2014) and litter
86 decomposition (Bélanger et al., 2019) suggesting that microclimate, as well as macroclimate,
87 regimes may influence how microbial community function responds to contemporary and future
88 variation in environmental conditions.

89 In this study we take an experimental approach to disentangle whether the climatic
90 regime influences decomposition rates via direct effects on microbial activities only, or
91 additionally via indirect effects mediated by functional legacies that are embedded within the
92 climate regime. We first look for evidence that site-level macroclimate regimes generate

93 microbial communities that function distinctly. Second, we test competing hypotheses, the first
94 of which is based on the idea that microclimate variation within sites does not generate
95 functional legacies because they would be overwhelmed by rates of local dispersal of microbes
96 and/or materials (e.g., decomposing leaves; Allison and Martiny 2008; Nemergut et al. 2013).
97 Alternatively, high within-site heterogeneity in microclimate could allow functional legacies to
98 manifest at local scales, generating microbial communities with distinct functional responses to
99 contemporary moisture conditions. Our laboratory microcosm approach established and
100 controlled three contemporary soil moisture regimes, imposed on a common leaf litter inoculated
101 with soil microbial communities sourced from local-scale spatial gradients in soil moisture
102 regime found within two forest sites within a regional climate gradient. We repeatedly measured
103 carbon mineralization of the litter for 202 days.

104 **Materials and Methods**

105 ***Microsite characteristics and sampling***

106 We worked at two forest sites, ~650 km apart, that are part of the National Ecological
107 Observation Network (NEON), which splits the continental United States into 20 ecoclimate
108 domains to monitor ecosystems under environmental change across time and space (Keller et al.,
109 2008). Both sites are temperate deciduous forests that spanned from the mid-Atlantic domain
110 (SCBI: Smithsonian Conservation Biological Institute, Front Royal, VA) to the Northeast
111 domain (HARV: Harvard Forest, Petersham, MA). The two sites have different climate and soil
112 characteristics (Table 1) and differ in the degree to which soil moisture varies within each site
113 (Fig. 1). Within each forest site we established twenty-seven microsites (1 m^2) around the
114 perimeter of the eddy-flux tower footprint, which covers about 1.3 km^2.

Microsites were on average 46 m apart from the next nearest microsite with the closest two microsites being 18 m apart and the two microsites furthest from one another being 1,389 m apart within a site. We chose microsites that varied in topographic position (e.g., ridge versus valley bottom) to capture heterogeneity in microsite conditions. Microclimate measurements were taken at three discrete time points over a 10-month period from December 2019 to September 2020. Temperature was measured at 5 cm depth for soil and 1 cm depth for the litter layer using a hand-held thermometer. Soil volumetric moisture was measured in the field using a time domain reflectometry (TDR) probe, inserted at a 45° angle to ~5 cm depth, in addition to gravimetric moisture measured in the lab. These discrete point measurements were intended to capture relative differences in soil characteristics over space, specifically for soil moisture, which has often been described as temporally stable where relative moisture differences in sampled locations persist over time (Vachaud et al., 1985; Brocca et al., 2010; Penna et al., 2013). In our study, temporal stability calculated through Spearman's rank-order correlation reveals high temporal stability in gravimetric soil moisture ($r_s > 0.73$) for the three point measurements over the year, confirming that point measurements are useful for characterizing spatial patterns in soil variables such as relative moisture regimes (Vanderlinden et al., 2012).

Leaf litter was collected at peak litter fall in November 2019 across all of the microsites. Due to its presence across both sites, northern red oak (*Quercus rubra* L.) litter was pooled to create a common litter substrate and air dried. The *Q. rubra* leaves were ground to 2 mm using a Wiley mill, further mixed to homogenize the sample, and then autoclaved twice at 121 °C at 15 psi for 20 min, following the approach of Strickland et al. (2009a, b; Keiser et al. 2011) to sterilize the litter. The top 5 cm of soil was sampled with a 2-cm dia. corer at each microsite in December 2019 for HARV and January 2020 for SCBI. Five to ten cores were taken per

138 microsite, passed through a 4-mm sieve, then homogenized and stored at 4 °C until their use as
139 the microbial community inoculum (see next section).
140 Soils were similarly sampled at each microclimate measurement point. Specifically,
141 gravimetric soil moisture (GWC) was measured by drying soils for 24 h at 105 °C and is
142 reported as the percent water contained in field fresh soil. Water holding capacity (WHC) was
143 measured for the soils and sterilized litter by allowing saturated samples to drain for 2 h in
144 Whatman #1 filter paper and then to dry for 24 h at 105 °C. Soil pH was measured by placing
145 soil in deionized water (1:1 volumetric ratio), followed by measurement of the supernatant with a
146 benchtop pH meter after 10 min. Microbial biomass was assayed using a modified substrate
147 induced respiration (SIR) method (Fierer et al., 2003; Strickland et al., 2010) whereby 5 mL of
148 soil was incubated at 20 °C with autolyzed yeast. After 1 h of gentle shaking, headspaces were
149 flushed with CO_2-free air, and then accumulated headspace CO_2 was measured after 4 h with an
150 infrared gas analyzer (IRGA; Model LI-7000, Li-Cor Biosciences, Lincoln, Nebraska, USA).
151 SIR biomass is reported as maximum CO_2 production normalized by dry weight equivalent of
152 soil. Volume, as opposed to mass, was used to determine the amount of soil for the SIR
153 incubations because of marked differences in soil organic matter contents (which causes similar
154 masses to have very different volumes). Total soil carbon and nitrogen were measured on air-
155 dried soils by grinding, packing in tins and combusting them on an NA1500 CHN Analyzer
156 (Carlo Erba Strumentazione, Milan, Italy).
157 ***Microcosm set-up***
158 Our microcosm design followed published approaches (Strickland et al., 2009a, b; Keiser et al.,
159 2011; Cleveland et al., 2014) that introduce a small amount of soil, to serve as a microbial
160 inoculum, to a litter environment which serves as the dominant organic substrate across the

161 incubation. The approach then standardizes the substrate (i.e., the litter) and varies the microbial
162 community inoculum, to tease out whether communities function similarly or differently once
163 placed in a standard environment. Specifically, we used 50-mL centrifuge tubes with 0.25 g of
164 dry weight equivalent soil from each microsite, which was thoroughly mixed with 1-g dry-
165 weight equivalent and ground *Q. rubra* litter. Soil-only controls were constructed that contained
166 ~6 g dry-weight equivalent soil, which were used to correct C mineralization fluxes from the leaf
167 litter by subtracting the C mineralized throughout the experiment from the soil. The estimated
168 respiration from the soil in the soil-litter microcosms was, at most, 10.6% and the mean was 2.3
169 ± 1.6% (SD) of the cumulative CO_2 respired per microcosm.
170 Three treatments were applied to the soil only and soil+litter microcosms to create
171 constant moisture regimes ('Lab Moisture') that spanned from drier (35% WHC) to mesic (60%
172 WHC) to wet (100% WHC) conditions. WHC for the litter+soil mixtures was obtained by
173 measuring WHC for the ground litter and soils as described above and calculating target
174 moisture content based on the dry mass equivalents for the litter and soil. In total, 162 unique
175 soil-litter mixtures were created (2 sites × 27 composite soils from each microsite × 3 lab
176 moisture treatments) and were maintained at target moisture by mass adjustments with weekly
177 DI-water additions. The additional 162 soil-only microcosms were also incubated under the same
178 three lab moisture regimes. All microcosms were kept at 20 °C over the course of the
179 experiment. Carbon mineralization was measured over 202 days by measuring CO_2 production in
180 each microcosm over 24 h at 17 time points (day 1, 6, 9, 13, 20, 27, 34, 43, 50, 64, 78, 92, 105,
181 120, 141, 168, 202) with the frequency of measurement decreasing over the course of the
182 experiment. At each time point, a cap with a rubber septum and O-ring was fitted to the top of
183 the 50-mL tube and the headspace flushed with CO_2-free air. After 24 h of incubation, a 5-mL

184 sample of gas was taken and used to flush a 1-mL sample loop that was then transferred for
185 measurement on an IRGA.
186 To assess variability of C mineralization of the same litter-soil mix under different
187 conditions, we captured the distribution of responses from a subset of the unique litter-soil mixes
188 through high replication. This approach can be useful for representing error in measurements and
189 for propagating parameter uncertainties into modeling frameworks (LeBauer et al., 2013). Here,
190 one microsite was selected from dry and wet field moisture conditions at each site and replicated
191 7 times under each treatment (4 soils × 7 replicates × 3 lab moisture treatments = 84
192 microcosms). Together with the experimental units (164) and soil controls (164), we maintained
193 408 microcosms across the 202-day experiment.
194 ***Data and inferential analysis***
195 Cumulative C mineralization rates were calculated using the area under the curve ('AUC')
196 function in the DescTools package (Signorell, 2021) in the statistical freeware R (R Core Team,
197 2020). To estimate CO_2 evolved from *Q. rubra* litter, cumulative C mineralization from litter-soil
198 microcosms were subtracted from soil-only controls for the corresponding microsite soil sample.
199 Differences in cumulative C mineralization between the two sites and lab moisture treatment
200 were analyzed using ANOVA and comparisons were assessed using Tukey's honest significance
201 test.
202 To directly test the competing hypotheses that decomposer community response to
203 contemporary moisture conditions are or are not modified by historical soil moisture
204 microclimate, we used regression to model experimental moisture treatment with known controls
205 on litter decomposition – via microbial functional legacies – such as field soil moisture,
206 temperature, and soil pH (Table 2). This causal statistical inferential approach follows Holland

(1986), where the focus is on identifying the conditional effect size of a causal variable relative to other known causes (see Bradford et al. 2021). Cumulative respiration response was natural-log transformed to meet assumptions of normality, but results were qualitatively the same with non-transformed data. We first ran a linear model including only gravimetric soil moisture ('Field Soil Moisture'), treatment ('Lab Moisture'), and their interaction (Reduced Model, Table S1). A second-order term for Lab Moisture was included because of the expectation that microbial communities will have a unimodal response, where mesic (60% WHC) conditions will have the highest mineralization rates (Howard and Howard, 1993). We ran 'Lab Moisture' as a continuous variable to allow comparison with 'Field Soil Moisture' at the same scale and assess relative effect sizes. Variables were standardized by subtracting the mean and dividing by one standard deviation to allow comparison of relative effects when adding variables with different units. When we included site in the models, variables were standardized by subtracting the mean and dividing by two standard deviations to assess continuous and binary predictors ('Site') on the same scale (Gelman, 2008).

Among the reduced and full models, we iteratively included and omitted interactions and non-correlated variables to explore the degree to which the effect sizes of our variables of interest ('Field Soil Moisture' and 'Lab Moisture') were influenced by model structure (Fig. S1). This sensitivity analysis approach is tailored to test the robustness of the absolute and relative causal effect sizes of the predictors of interest, in light of the fact that ecological outcomes are multi-causal and conditional, with plausible causative variables typically non-orthogonal (see Hobbs et al. 2012 and Bradford et al. 2019). The variables used in the model for both sites and for each site included soil pH, soil temperature, litter temperature, and soil bulk density. In addition to including variables that were not or only marginally correlated with field soil

moisture, we examined how inferences about soil moisture regime might be influenced by related microsite conditions such as total soil organic C (TOC) concentration and microbial biomass that also can influence microbial function. Unstandardized model results and those of the sensitivity analyses are included in the supplementary material (Table S2; Figs. S1-2). R package 'tidyverse' (Wickham et al., 2019) was used to process data and for visualization; 'jtools' (Long, 2020), 'interactions' (Long, 2019), and 'sjPlot' (Lüdecke, 2021) were used to report and visualize model analyses.

Results

Site comparisons

We found functional differences between soil communities from the two sites, but the strength of the difference was dependent on contemporary moisture conditions (Table 2). Specifically, cumulative C mineralization in the dry conditions was 110.3 ± 5.1 mg C g^{-1} litter (mean ± SE) for the SCBI soils, which is 97% higher than the cumulative mineralization observed for the HARV soil communities (55.7 ± 2.5 mg C g^{-1} litter; Fig. 2d). In mesic conditions, SCBI communities mineralized only 24% more litter C than the corresponding HARV communities (74.1 ± 3.5 mg C g^{-1} litter compared to 59.7 ± 2.0 mg C g^{-1} litter), whereas under the wet conditions, mean cumulative mineralization for SCBI was 4% higher than HARV (53.8 ± 1.4 mg C g^{-1} litter compared to 51.9 ± 1.3 mg C g^{-1} litter; Fig. 2f).

The differences between the sites and among the lab treatments were underlain by differences in temporal dynamics over the 202-day incubation, which translated to different cumulative mineralization rates (Fig. 2d-f). Carbon mineralization rates from leaf litter increased and peaked in all treatments across the first six to nine days of the incubations (Fig. 2). Decomposer communities from HARV across treatments exhibited a single peak respiration after

six to nine days. SCBI communities exhibited a second, delayed increase in respiration that varied in magnitude and length depending on laboratory treatment: dry conditions produced a large response which began at day 43 and peaked at day 105 (Fig. 2a); mesic conditions exhibited a second, smaller peak at 27 days (Fig. 2b); and the wet conditions had a second peak at day 34 that was similar in magnitude to the first peak (Fig. 2c). These secondary peaks in C mineralization rates for the SCBI soils in the two drier lab treatments meant that the expectation that cumulative respiration rates would peak at 60% WHC – as they did for HARV soil inocula (Figs. 2d-f) – was not realized for the SCBI soil communities. Instead, the main effect of lab moisture treatment for the both-sites model was negative (Table 2). Notably, however, the standardized coefficient for the interaction between lab moisture and the field moisture conditions was approximately three-fourths the size of the lab moisture main effect (Both Sites, Table 2). This large interaction effect most likely arose because in the dry and mesic lab treatments, drier soils from SCBI resulted in higher cumulative mineralization than from wetter soils from HARV, whereas the wet treatment had similar cumulative fluxes when the two sites were compared (Figs. 2d-f). The large coefficient for Site was likely driven by these high cumulative mineralization rates for SCBI inocula in the dry and mesic lab-moisture treatments, which overall led to higher cumulative mineralization (across all lab treatments) for SCBI versus HARV inocula.

Harvard Forest, MA – HARV

Functional differences among the soil decomposer communities, associated with the field moisture conditions from where they were sourced, were similarly observed when the HARV data were considered independent of the SCBI data. Specifically, there was a main effect of field soil moisture and an interactive effect with lab moisture treatment (Table 2). The imposed lab

moisture regime did not have a strong effect, but the relatively large, negative second-order Lab Moisture term reflects the observation that the highest cumulative mineralization rates were under mesic moisture conditions. The effect of field soil moisture and the interaction with lab moisture treatment drove the majority of variation in this site as indicated by the standardized coefficient terms. Notably, the 'Field Soil Moisture' terms reveal that the soil communities from across the different microsite moisture regimes at the HARV site are functionally distinct. Notably, these functional differences had a larger effect on the observed mineralization rates than the lab-imposed moisture conditions.

The interaction term appeared to be associated with the fact that soil communities sourced from drier microsites had lower cumulative mineralization rates under the drier lab moisture treatment, whereas for soil communities sourced from the wettest microsites cumulative mineralization was lowest under the wettest lab moisture treatment (Fig. 3a). These dynamics meant that the field moisture regime had a strong positive effect on cumulative respiration rates for the dry lab treatment, but a much shallower slope for the wet lab treatment (Fig. 3a). The slope for the mesic lab treatment was intermediate but, again, communities sourced from increasingly moist microclimate regimes had higher cumulative respiration rates than those sourced from drier field regimes (Fig. 3a). Using the regressions from Table 2 and Fig 3, we estimated the effect size that history of soil moisture had on contemporary responses. In dry lab conditions (Fig. 3a), communities from the wetter end of the moisture gradient mineralized 89% more litter C than soils from drier microclimate regimes: 39.0 ± 3.7 mg C g^{-1} litter compared to 73.6 ± 3.9 mg C g^{-1} litter. Under mesic conditions (Fig. 3a), communities sourced from wetter microclimates mineralized 50% more than dry microclimates: 48.2 ± 2.8 mg C g^{-1} litter compared to 72.0 ± 2.9 mg C g^{-1} litter. The wet lab treatment (Fig 3a, blue solid-line) resulted in

299 soils from the wettest microclimates mineralizing 14% more C compared to soils from drier
300 microclimates: 48.7 ± 3.9 mg C g^{-1} litter compared to 55.4 ± 4.2 mg C g^{-1} litter. Notably, the
301 within-site variation across the field soil moisture gradient is comparable to the differences in
302 mineralization rates between sites under dry conditions: 89% difference within HARV vs. 97%
303 between sites. Further, the difference in cumulative respiration from the microsite communities
304 that were incubated under mesic lab conditions were higher within the HARV site than between
305 the two forest sites (50% variation within HARV microsites vs. 24% variation between HARV
306 and SCBI sites).

307 ***Smithsonian Conservation Biological Institute, VA – SCBI***

308 Decomposer communities from the SCBI site were not influenced by their local historical
309 moisture regimes (Table 1, Fig 3b). The slopes for cumulative respiration for lab moisture
310 treatments were not significantly different suggesting that there were no within-site differences
311 in microbial function. Standardized effect size estimates for field soil moisture ranged from 0 to
312 0.10 which indicates that there is potentially a positive association of field soil moisture regime
313 with cumulative C mineralization, but the interaction between lab and field moisture essentially
314 had a slope of zero (Table 2). As a result, the lab-based moisture treatments accounted for nearly
315 all of the variation in cumulative C mineralization that was observed (SCBI: 'Lab Moisture',
316 Table 2, Fig. 3b). Dry conditions resulted in mineralization rates of 110 ± 5.1 mg C g^{-1} litter
317 (mean ± SE): 49% higher than mesic conditions (74.1 ± 3.5 mg C g^{-1} litter) and 105% higher
318 than wet conditions (53.8 ± 1.4 mg C g^{-1} litter).

319 ***Model structural sensitivity***

320 Given that the microsites from where we sourced the soil communities differed in more than
321 moisture, we evaluated how other microenvironmental predictors that might influence microbial

community functioning affected our interpretation of field moisture history as a causal variable. We explored how the addition of factors not strongly correlated with soil moisture, such as soil pH and soil temperature, affected the coefficient estimates of interest (Table 2). For the both site model, HARV, and SCBI models, coefficient sizes for 'Field Soil Moisture' remained relatively unchanged compared to a reduced model with only 'Field Soil Moisture' and 'Lab Moisture' (Table S1). Microbial biomass and TOC were highly correlated with field soil moisture (respectively, $r = 0.67$ and 0.89 for HARV and 0.68 and 0.91 for SCBI; SI Tables 3, 4), with variance inflation factors (VIF) > 2 when included in main effects models. For the models including both sites and only HARV, the inclusion of these variables continued to not affect the sign and magnitude of the 'Field Soil Moisture' effects (Fig. S1c). In the model specified for SCBI, the inclusion of TOC modified the coefficient for field soil moisture but it remained insignificant and close to zero (Fig. S1e). Across all models, we lastly substituted measures of field soil moisture taken at different times, and the mean value of these over the three time points. Soil moisture across sampled time points provided coefficient estimates that support our conclusions (Figs. S2a-e). In short, our results appeared relatively insensitive to model structural and parameter assumptions, suggesting that the coefficient estimates for 'Field Soil Moisture' and 'Lab Moisture' were robust.

To understand how unique experimental units might vary if they themselves were replicated, we replicated microcosms from one wet and one dry microsite within each site (4 microsites × 3 treatments × 8 replicates). Variation within these subsamples had a median coefficient of variation (COV) of 12%, which was consistently lower than the variation within treatments and site groupings except for a single highly-replicated SCBI community under dry conditions. Overall, within-replicate variation in C mineralization was about half that of within-

345 site variation across treatments providing confidence that our conclusions about laboratory
346 moisture treatment and microsite legacy effects are robust to potential within-replicate variation
347 in observed C mineralization rates.

348 **Discussion**

349 Numerous studies report that soil communities sampled from sites with different precipitation
350 regimes (and hence assumed differences in soil moisture regimes) exhibit functionally distinct
351 responses to contemporary moisture conditions (Evans and Wallenstein, 2012; Hawkes et al.,
352 2017). Our site-level findings contribute a further empirical example where our two sites, HARV
353 and SCBI, had distinct C mineralization time-courses and cumulative fluxes across different lab-
354 imposed moisture regimes (Fig. 2). This finding supports regional studies that observe that
355 microbial responses to new conditions can be shaped by environmental history (Evans and
356 Wallenstein, 2012; Averill et al., 2016; Hawkes et al., 2017; Glassman et al., 2018). We
357 additionally asked whether these macroscale functional differences were exhibited at local,
358 within-site scales. We found evidence for both of our hypotheses where, in one site (HARV),
359 historical microsite conditions were associated with differences in cumulative C mineralization.
360 Whereas in the other site (SCBI) only lab-imposed moisture conditions drove differences in C
361 mineralization with no evidence of within-site differences in functioning.

362 Differences in microbial function emerge from multiple controls such as environmental
363 history and contemporary conditions. We specifically asked how within-site heterogeneity in soil
364 moisture regimes might generate microbial functional differences. In HARV, soils sourced from
365 wetter microclimates mineralized more litter C than soils from drier microclimates across all lab-
366 imposed moisture conditions (Fig. 3a). This effect was stronger for the dry and mesic lab
367 moisture conditions compared to the wet lab conditions (Table 3; Fig. 3a). Results from this site

suggest historical legacies of soil moisture shape the functioning of communities at local scales, reflecting similar functional patterns across regional precipitation gradients where historically wetter sites exhibit higher respiration rates (Hawkes et al., 2017, 2020). Whereas dispersal limitation, landscape heterogeneity and adaptation can play a role in functional divergence across broad spatial extents (Talbot et al., 2014; Strickland et al., 2015; Maynard et al., 2019), patterns revealed here also suggest that within-site, spatial heterogeneity in environmental conditions can generate functionally different microbial communities.

Drier moisture regimes can lead to lower microbial biomass but select for taxa that are more resistant to moisture stress and lead to higher functional ability under stressful conditions (Lennon et al., 2012; Maynard et al., 2019; Lustenhouwer et al., 2020). This broad scale pattern was observed between the two sites, where the SCBI soil communities, that generally experience a drier soil moisture regime (Fig. 1), also exhibited much higher mineralization rates than the HARV soil communities under dry lab-moisture conditions (Figs. 2d, 3). However, the highest mineralization rates for the HARV soil communities were always observed for communities sourced from wetter microclimates, and the greatest among-community sensitivity to contemporary moisture conditions was observed under dry lab conditions (Fig. 3a). This within-site pattern observed at HARV was distinct from the within-site SCBI pattern (Fig. 3), and these within-site patterns were distinct from the patterns observed between sites. Collectively, our results suggest that functional differences observed among sites at regional scales do not necessarily translate to finer scales, raising the possibility that mechanisms that generate microbial functional differences at one scale might be distinct to mechanisms operating at another scale.

390 In contrast to the HARV observations, within the SCBI site we observed functionally
391 equivalent decomposer communities where C mineralization rates were driven almost entirely by
392 the lab moisture conditions (Table 2; Fig. 3b). Both forest sites experience similar amounts of
393 annual precipitation, but the warmer mean climate of SCBI contributes to lower soil moisture
394 values and a narrower spatial range in field-soil moisture regimes (Fig. 1, Table 1; CV = 0.191
395 for SCBI compared to 0.261 for HARV). Although results from SCBI do not show a strong
396 effect of within-site moisture, as found at HARV, the effect size was still positive (Table 2). This
397 positive coefficient suggests that there was also a positive effect of field soil moisture regime at
398 this site, but it had only a small influence on mineralization rates. The microbial functional
399 response of the SCBI soil communities to lab moisture conditions were, however, unexpected.
400 Specifically, communities under dry lab conditions had higher C mineralization than
401 communities under mesic and wet moisture lab conditions (Fig. 2 and 3b). This empirical result
402 provides further evidence that microbial respiration does not always peak at mesic moisture
403 conditions (Moyano et al., 2013). A potential explanation for the drier conditions under which
404 we observed the peak is that, in leaf litter, constraints on C mineralization rates due to lower
405 moisture may be smaller than in soil due to better gas and nutrient diffusion in dense litter packs.
406 Nevertheless, the peak mineralization for the SCBI communities was still drier than for the
407 HARV communities. Whereas we did not uncover the specific mechanisms explaining this
408 observation, adaptation to drier conditions across the two sites and within SCBI reflect evidence
409 from other systems where drier sites exhibit higher functional potentials. For example, Averill et
410 al. (2016) found that enzyme potentials were linked to historical precipitation and soil moisture,
411 with historically drier sites exhibiting stronger enzyme activity and sensitivity to moisture.
412 Similarly, in our study, historical moisture regimes beget unique functional microbial responses

413 that can lead to deviations from the typical unimodal response of mineralization to contemporary
414 moisture conditions.

415 Models that represent explicitly how microorganisms mediate decomposition aim to
416 explore how changes in environmental conditions affect microbes and in turn the rates of the
417 biogeochemical processes they mediate (Wang et al., 2013; Wieder et al., 2013; Abramoff et al.,
418 2018). These process-based models are an ideal framework for querying how functional legacies
419 might affect rates. Our study is a starting point in addressing how functional legacies between
420 and within sites might affect biogeochemical rates as moisture changes seasonally and
421 interannually through climate change. For example, these models typically assume a unimodal
422 moisture response, such that increasing moisture increases decomposition up to a threshold
423 where decomposition rate decreases again (Davidson et al., 2012). We did observe this pattern at
424 HARV, for the lab moisture treatments that were imposed, but not at SCBI suggesting that
425 functional legacies create context-dependency in how contemporary moisture controls litter-C
426 mineralization rates. Certainly, our data still support the assumption that contemporary moisture
427 exerts strong direct control on mineralization rates, but equally our lab experiment provides
428 further justification for field experiments that address how historical moisture regimes modify
429 these contemporary responses. Experimental studies that tease out microbial functional effects
430 from other environmental effects can help quantify the influence of functional microbial
431 differences on contemporary biogeochemical process rates (Hawkes et al., 2017; Glassman et al.,
432 2018). When partnered with process-based models that represent microbial functional
433 differences, such experimental observations can help inform how functional differences might
434 affect biogeochemical process rates under new conditions (Wieder et al., 2015a; Hall et al., 2018;
435 Malik et al., 2020; Wang and Allison, 2021).

As more research focuses on the role of microbial biogeography, diversity and its relation to ecosystem function, our data reveal that the nature of these relationships are likely to be strongly scale- and context-dependent. Certainly, our data contribute to previous findings that historical contingencies shape contemporary functioning when sites are compared at regional scales. As such, they bolster expectations that measuring community functional potentials at the regional scale captures community adaptation to climatic drivers at similar scales (Strickland et al., 2015; Maynard et al., 2019). Yet our data also reveal that pronounced differences in field microclimate regime equally can affect microbial function under contemporary moisture conditions, in a manner distinct from those observed to arise because of macroclimate regimes. These scale dependencies might be expected to generate unique, non-linear, emergent responses of biogeochemical process rates to changing moisture conditions at regional scales, highlighting the importance of evaluating their influence on projections of climate change impacts on C cycling.

Acknowledgements

All research was supported by the U.S. National Science Foundation under the Macrosystems Biology and NEON-Enabled Science program, through grants DEB-1926482 and DEB-1926413. WRW was supported by the U.S. Department of Energy under award number BSS DE-SC0016364. We thank Ella Bradford, Ashley Keiser, Michael Maier and James Dalton Maier for their help during field collection. We also thank Audrey Barker Plotkin and Greg Chapman for site support.

457

458 ***Data availability and supplementary information***

459 Data and code are available on DataDryad https://doi.org/10.5061/dryad.51c59zw8j.

460

461 **References**

462 Abramoff, R., Xu, X., Hartman, M., O'Brien, S., Feng, W., Davidson, E., Finzi, A., Moorhead,
463 D., Schimel, J., Torn, M., Mayes, M.A., 2018. The Millennial model: in search of
464 measurable pools and transformations for modeling soil carbon in the new century.
465 Biogeochemistry 137, 51–71. doi:10.1007/s10533-017-0409-7

466 Aerts, R., 1997. Climate, leaf litter chemistry and leaf litter decomposition in terrestrial
467 ecosystems: a triangular relationship. Oikos 79, 439–449.

468 Allison, S.D., Martiny, J.B.H., 2008. Resistance, resilience, and redundancy in microbial
469 communities. Proceedings of the National Academy of Sciences 105, 11512–11519.
470 doi:10.1073/pnas.0801925105

471 Averill, C., Waring, B.G., Hawkes, C.V., 2016. Historical precipitation predictably alters the
472 shape and magnitude of microbial functional response to soil moisture. Global Change
473 Biology 22, 1957–1964. doi:10.1111/gcb.13219

474 Baldrian, P., 2014. Distribution of Extracellular Enzymes in Soils: Spatial Heterogeneity and
475 Determining Factors at Various Scales. Soil Science Society of America Journal 78, 11–
476 18. doi:10.2136/sssaj2013.04.0155dgs

477 Baldrian, P., Merhautová, V., Petránková, M., Cajthaml, T., Šnajdr, J., 2010. Distribution of
478 microbial biomass and activity of extracellular enzymes in a hardwood forest soil reflect

soil moisture content. Applied Soil Ecology 46, 177–182. doi:10.1016/j.apsoil.2010.08.013

Baveye, P.C., Otten, W., Kravchenko, A., Balseiro-Romero, M., Beckers, É., Chalhoub, M., Darnault, C., Eickhorst, T., Garnier, P., Hapca, S., Kiranyaz, S., Monga, O., Mueller, C.W., Nunan, N., Pot, V., Schlüter, S., Schmidt, H., Vogel, H.-J., 2018. Emergent Properties of Microbial Activity in Heterogeneous Soil Microenvironments: Different Research Approaches Are Slowly Converging, Yet Major Challenges Remain. Frontiers in Microbiology 9, 1929. doi:10.3389/fmicb.2018.01929

Bélanger, N., Collin, A., Ricard-Piché, J., Kembel, S.W., Rivest, D., 2019. Microsite conditions influence leaf litter decomposition in sugar maple bioclimatic domain of Quebec. Biogeochemistry 145, 107–126. doi:10.1007/s10533-019-00594-1

Bond-Lamberty, B., Thomson, A., 2010. Temperature-associated increases in the global soil respiration record. Nature 464, 579–582. doi:10.1038/nature08930

Bradford, M.A., McCulley, R.L., Crowther, T.W., Oldfield, E.E., Wood, S.A., Fierer, N., 2019. Cross-biome patterns in soil microbial respiration predictable from evolutionary theory on thermal adaptation. Nature Ecology & Evolution 3, 223–231. doi:10.1038/s41559-018-0771-4

Bradford, M.A., Veen, G.F., Bonis, A., Bradford, E.M., Classen, A.T., Cornelissen, J.H.C., Crowther, Thomas.W., De Long, J.R., Freschet, G.T., Kardol, P., Manrubia-Freixa, M., Maynard, D.S., Newman, G.S., Logtestijn, R.S.P., Viketoft, M., Wardle, D.A., Wieder, W.R., Wood, S.A., van der Putten, W.H., 2017. A test of the hierarchical model of litter decomposition. Nature Ecology & Evolution 1, 1836–1845. doi:10.1038/s41559-017-0367-4

Bradford, M.A., Warren II, R.J., Baldrian, P., Crowther, T.W., Maynard, D.S., Oldfield, E.E., Wieder, W.R., Wood, S.A., King, J.R., 2014. Climate fails to predict wood decomposition at regional scales. Nature Climate Change 4, 625–630. doi:10.1038/nclimate2251

Bradford, M.A., Wood, S.A., Addicott, E.T., Fenichel, E.P., Fields, N., González-Rivero, J., Jevon, F.V., Maynard, D.S., Oldfield, E.E., Polussa, A., Ward, E.B., Wieder, W.R., 2021. Quantifying microbial control of soil organic matter dynamics at macrosystem scales. Biogeochemistry 1–22. doi:10.1007/s10533-021-00789-5

Brocca, L., Melone, F., Moramarco, T., Morbidelli, R., 2010. Spatial-temporal variability of soil moisture and its estimation across scales. Water Resources Research 46, 1–14. doi:10.1029/2009WR008016

Cleveland, C.C., Reed, S.C., Keller, A.B., Nemergut, D.R., O'Neill, S.P., Ostertag, R., Vitousek, P.M., 2014. Litter quality versus soil microbial community controls over decomposition: a quantitative analysis. Oecologia 174, 283–294. doi:10.1007/s00442-013-2758-9

Crowther, T.W., van den Hoogen, J., Wan, J., Mayes, M.A., Keiser, A.D., Mo, L., Averill, C., Maynard, D.S., 2019. The global soil community and its influence on biogeochemistry. Science 365, eaav0550. doi:10.1126/science.aav0550

Davidson, E.A., Samanta, S., Caramori, S.S., Savage, K., 2012. The Dual Arrhenius and Michaelis-Menten kinetics model for decomposition of soil organic matter at hourly to seasonal time scales. Global Change Biology 18, 371–384. doi:10.1111/j.1365-2486.2011.02546.x

Evans, S.E., Wallenstein, M.D., 2014. Climate change alters ecological strategies of soil bacteria. Ecology Letters 17, 155–164. doi:10.1111/ele.12206

525 Evans, S.E., Wallenstein, M.D., 2012. Soil microbial community response to drying and
526 rewetting stress: does historical precipitation regime matter? Biogeochemistry 109, 101–
527 116. doi:10.1007/s10533-011-9638-3
528 Falkowski, P.G., Fenchel, T., Delong, E.F., 2008. The Microbial Engines That Drive Earth's
529 Biogeochemical Cycles. Science 320, 1034–1039. doi:10.1126/science.1153213
530 Fatichi, S., Manzoni, S., Or, D., Paschalis, A., 2019. A Mechanistic Model of Microbially
531 Mediated Soil Biogeochemical Processes: A Reality Check. Global Biogeochemical
532 Cycles 33, 620–648. doi:10.1029/2018GB006077
533 Fierer, N., Schimel, J.P., Holden, P.A., 2003. Variations in microbial community composition
534 through two soil depth profiles. Soil Biology and Biochemistry 35, 167–176.
535 doi:10.1016/S0038-0717(02)00251-1
536 Gelman, A., 2008. Scaling regression inputs by dividing by two standard deviations. Statistics in
537 Medicine 27, 2865–2873. doi:10.1002/sim.3107
538 Glassman, S.I., Weihe, C., Li, J., Albright, M.B.N., Looby, C.I., Martiny, A.C., Treseder, K.K.,
539 Allison, S.D., Martiny, J.B.H., 2018. Decomposition responses to climate depend on
540 microbial community composition. Proceedings of the National Academy of Sciences
541 115, 11994–11999. doi:10.1073/pnas.1811269115
542 Hall, E.K., Bernhardt, E.S., Bier, R.L., Bradford, M.A., Boot, C.M., Cotner, J.B., del Giorgio,
543 P.A., Evans, S.E., Graham, E.B., Jones, S.E., Lennon, J.T., Locey, K.J., Nemergut, D.,
544 Osborne, B.B., Rocca, J.D., Schimel, J.P., Waldrop, M.P., Wallenstein, M.D., 2018.
545 Understanding how microbiomes influence the systems they inhabit. Nature
546 Microbiology 3, 977–982. doi:10.1038/s41564-018-0201-z

547 Hawkes, C.V., Shinada, M., Kivlin, S.N., 2020. Historical climate legacies on soil respiration
548 persist despite extreme changes in rainfall. Soil Biology and Biochemistry 143, 107752.
549 doi:10.1016/j.soilbio.2020.107752
550 Hawkes, C.V., Waring, B.G., Rocca, J.D., Kivlin, S.N., 2017. Historical climate controls soil
551 respiration responses to current soil moisture. Proceedings of the National Academy of
552 Sciences 114, 6322–6327. doi:10.1073/pnas.1620811114
553 Hobbs, N.T., Andrén, H., Persson, J., Aronsson, M., Chapron, G., 2012. Native predators reduce
554 harvest of reindeer by Sámi pastoralists. Ecological Applications 22, 1640–1654.
555 Holland, P.W., 1986. Statistics and Causal Inference. Journal of the American Statistical
556 Association 81, 945–960. doi:10.1080/01621459.1986.10478354
557 Howard, D.M., Howard, P.J.A., 1993. Relationships Between CO2 Evolution, Moisture Content
558 and Temperature for a Range of Soil Types. Soil Biology and Biochemistry 25, 1537–
559 1546. doi:10.1016/0038-0717(93)90008-Y
560 Karhu, K., Auffret, M.D., Dungait, J.A.J., Hopkins, D.W., Prosser, J.I., Singh, B.K., Subke, J.-
561 A., Wookey, P.A., Ågren, G.I., Sebastià, M.-T., Gouriveau, F., Bergkvist, G., Meir, P.,
562 Nottingham, A.T., Salinas, N., Hartley, I.P., 2014. Temperature sensitivity of soil
563 respiration rates enhanced by microbial community response. Nature 513, 81–84.
564 doi:10.1038/nature13604
565 Keiser, A.D., Strickland, M.S., Fierer, N., Bradford, M.A., 2011. The effect of resource history
566 on the functioning of soil microbial communities is maintained across time.
567 Biogeosciences 8, 1477–1486. doi:10.5194/bg-8-1477-2011

Keller, M., Schimel, D.S., Hargrove, W.W., Hoffman, F.M., 2008. A continental strategy for the National Ecological Observatory Network. Frontiers in Ecology and the Environment 6, 282–284. doi:10.1890/1540-9295(2008)6[282:ACSFTN]2.0.CO;2

Ladau, J., Eloe-Fadrosh, E.A., 2019. Spatial, Temporal, and Phylogenetic Scales of Microbial Ecology. Trends in Microbiology 27, 662–669. doi:10.1016/j.tim.2019.03.003

LeBauer, D.S., Wang, D., Richter, K.T., Davidson, C.C., Dietze, M.C., 2013. Facilitating feedbacks between field measurements and ecosystem models. Ecological Monographs 83, 133–154. doi:10.1890/12-0137.1

Lennon, J.T., Aanderud, Z.T., Lehmkuhl, B.K., Schoolmaster, D.R., 2012. Mapping the niche space of soil microorganisms using taxonomy and traits. Ecology 93, 1867–1879. doi:10.1890/11-1745.1

Loescher, H., Ayres, E., Duffy, P., Luo, H., Brunke, M., 2014. Spatial Variation in Soil Properties among North American Ecosystems and Guidelines for Sampling Designs. PLoS ONE 9, e83216. doi:10.1371/journal.pone.0083216

Long, J.A., 2020. jtools: Analysis and Presentation of Social Scientific Data.

Long, J.A., 2019. interactions: Comprehensive, User-Friendly Toolkit for Probing Interactions.

Lüdecke, D., 2021. sjPlot: Data Visualization for Statistics in Social Science.

Lustenhouwer, N., Maynard, D.S., Bradford, M.A., Lindner, D.L., Oberle, B., Zanne, A.E., Crowther, T.W., 2020. A trait-based understanding of wood decomposition by fungi. Proceedings of the National Academy of Sciences 117, 11551–11558. doi:10.1073/pnas.1909166117

589 Malik, A.A., Martiny, J.B.H., Brodie, E.L., Martiny, A.C., Treseder, K.K., Allison, S.D., 2020.
590 Defining trait-based microbial strategies with consequences for soil carbon cycling under
591 climate change. The ISME Journal 14, 1–9. doi:10.1038/s41396-019-0510-0
592 Maynard, D.S., Bradford, M.A., Covey, K.R., Lindner, D., Glaeser, J., Talbert, D.A., Tinker,
593 P.J., Walker, D.M., Crowther, T.W., 2019. Consistent trade-offs in fungal trait expression
594 across broad spatial scales. Nature Microbiology 4, 846–853. doi:10.1038/s41564-019-
595 0361-5
596 Maynard, D.S., Covey, K.R., Crowther, T.W., Sokol, N.W., Morrison, E.W., Frey, S.D., van
597 Diepen, L.T.A., Bradford, M.A., 2018. Species associations overwhelm abiotic
598 conditions to dictate the structure and function of wood-decay fungal communities.
599 Ecology 99, 801–811. doi:10.1002/ecy.2165
600 Moyano, F.E., Manzoni, S., Chenu, C., 2013. Responses of soil heterotrophic respiration to
601 moisture availability: An exploration of processes and models. Soil Biology and
602 Biochemistry 59, 72–85. doi:10.1016/j.soilbio.2013.01.002
603 Nemergut, D.R., Schmidt, S.K., Fukami, T., O'Neill, S.P., Bilinski, T.M., Stanish, L.F.,
604 Knelman, J.E., Darcy, J.L., Lynch, R.C., Wickey, P., Ferrenberg, S., 2013. Patterns and
605 Processes of Microbial Community Assembly. Microbiology and Molecular Biology
606 Reviews 77, 342–356. doi:10.1128/MMBR.00051-12
607 Parton, W., Silver, W.L., Burke, I.C., Grassens, L., Harmon, M.E., Currie, W.S., King, J.Y.,
608 Adair, E.C., Brandt, L.A., Hart, S.C., Fasth, B., 2007. Global-Scale Similarities in
609 Nitrogen Release Patterns During Long-Term Decomposition. Science 315, 361–364.
610 doi:10.1126/science.1134853

611 Penna, D., Brocca, L., Borga, M., Dalla Fontana, G., 2013. Soil moisture temporal stability at
612 different depths on two alpine hillslopes during wet and dry periods. Journal of
613 Hydrology 477, 55–71. doi:10.1016/j.jhydrol.2012.10.052
614 R Core Team, 2020. R: A Language and Environment for Statistical Computing. R Foundation
615 for Statistical Computing, Vienna, Austria.
616 Romero-Olivares, A.L., Allison, S.D., Treseder, K.K., 2017. Soil microbes and their response to
617 experimental warming over time: A meta-analysis of field studies. Soil Biology and
618 Biochemistry 107, 32–40. doi:10.1016/j.soilbio.2016.12.026
619 Schimel, J., Weintraub, M.N., 2003. The implications of exoenzyme activity on microbial carbon
620 and nitrogen limitation in soil: a theoretical model. Soil Biology and Biochemistry 35,
621 549–563. doi:10.1016/S0038-0717(03)00015-4
622 Signorell, A., 2021. DescTools: Tools for Descriptive Statistics.
623 Strickland, M.S., Devore, J.L., Maerz, J.C., Bradford, M.A., 2010. Grass invasion of a hardwood
624 forest is associated with declines in belowground carbon pools. Global Change Biology
625 16, 1338–1350. doi:10.1111/j.1365-2486.2009.02042.x
626 Strickland, M.S., Keiser, A.D., Bradford, M.A., 2015. Climate history shapes contemporary leaf
627 litter decomposition. Biogeochemistry 122, 165–174. doi:10.1007/s10533-014-0065-0
628 Strickland, M.S., Lauber, C., Fierer, N., Bradford, M.A., 2009a. Testing the functional
629 significance of microbial community composition. Ecology 90, 441–451. doi:10.1890/08-
630 0296.1
631 Strickland, M.S., Osburn, E., Lauber, C., Fierer, N., Bradford, M.A., 2009b. Litter quality is in
632 the eye of the beholder: initial decomposition rates as a function of inoculum
633 characteristics. Functional Ecology 23, 627–636. doi:10.1111/j.1365-2435.2008.01515.x

634 Šťursová, M., Bárta, J., Šantrůčková, H., Baldrian, P., 2016. Small-scale spatial heterogeneity of
635 ecosystem properties, microbial community composition and microbial activities in a
636 temperate mountain forest soil. FEMS Microbiology Ecology 92, fiw185.
637 doi:10.1093/femsec/fiw185
638 Swift, M.J., Heal, O.W., Anderson, J.M., 1979. Decomposition in terrestrial ecosystems, Studies
639 in Ecology. Univ of California Press.
640 Talbot, J.M., Bruns, T.D., Taylor, J.W., Smith, D.P., Branco, S., Glassman, S.I., Erlandson, S.,
641 Vilgalys, R., Liao, H.-L., Smith, M.E., Peay, K.G., 2014. Endemism and functional
642 convergence across the North American soil mycobiome. Proceedings of the National
643 Academy of Sciences 111, 6341–6346. doi:10.1073/pnas.1402584111
644 Vachaud, G., Passerat De Silans, A., Balabanis, P., Vauclin, M., 1985. Temporal Stability of
645 Spatially Measured Soil Water Probability Density Function. Soil Science Society of
646 America Journal 49, 822–828. doi:10.2136/sssaj1985.03615995004900040006x
647 van der Wal, A., Ottosson, E., de Boer, W., 2015. Neglected role of fungal community
648 composition in explaining variation in wood decay rates. Ecology 96, 124–133.
649 doi:10.1890/14-0242.1
650 Vanderlinden, K., Vereecken, H., Hardelauf, H., Herbst, M., Martínez, G., Cosh, M.H.,
651 Pachepsky, Y.A., 2012. Temporal Stability of Soil Water Contents: A Review of Data
652 and Analyses. Vadose Zone Journal 11. doi:10.2136/vzj2011.0178
653 Wang, B., Allison, S.D., 2021. Drought legacies mediated by trait trade-offs in soil microbiomes.
654 Ecosphere 12, 1–14. doi:10.1002/ecs2.3562

Wang, G., Post, W.M., Mayes, M.A., 2013. Development of microbial-enzyme-mediated decomposition model parameters through steady-state and dynamic analyses. Ecological Applications 23, 255–272. doi:10.1890/12-0681.1

Wickham, H., Averick, M., Bryan, J., Chang, W., McGowan, L.D., François, R., Grolemund, G., Hayes, A., Henry, L., Hester, J., Kuhn, M., Pedersen, T.L., Miller, E., Bache, S.M., Müller, K., Ooms, J., Robinson, D., Seidel, D.P., Spinu, V., Takahashi, K., Vaughan, D., Wilke, C., Woo, K., Yutani, H., 2019. Welcome to the {tidyverse}. Journal of Open Source Software 4, 1686. doi:10.21105/joss.01686.

Wieder, W.R., Allison, S.D., Davidson, E.A., Georgiou, K., Hararuk, O., He, Y., Hopkins, F., Luo, Y., Smith, M.J., Sulman, B., Todd-Brown, K., Wang, Y.-P., Xia, J., Xu, X., 2015a. Explicitly representing soil microbial processes in Earth system models: Soil microbes in earth system models. Global Biogeochemical Cycles 29, 1782–1800. doi:10.1002/2015GB005188

Wieder, W.R., Bonan, G.B., Allison, S.D., 2013. Global soil carbon projections are improved by modelling microbial processes. Nature Climate Change 3, 909–912. doi:10.1038/nclimate1951

Wieder, W.R., Grandy, A.S., Kallenbach, C.M., Taylor, P.G., Bonan, G.B., 2015b. Representing life in the Earth system with soil microbial functional traits in the MIMICS model. Geoscientific Model Development 8, 1789–1808. doi:10.5194/gmd-8-1789-2015

675 **Table 1** Site characteristics. Soil data are from the microsites within each site. Values represent
676 the mean of the microsites and standard deviation is displayed in parentheses for %C, %N, C:N,
677 Soil Moisture, Soil pH, and Microbial Biomass.

	Unit	Harvard Forest, MA (HARV)	Smithsonian Conservation Biological Institute, VA (SCBI)
Coordinates		(42.54, -72.17)	(38.89, -78.14)
Elevation	m a.s.l.	351	361
Mean Annual Temperature	°C	8	13
Mean Annual Precipitation	mm	976	1054
Soil C	%	23.9 (11.9)	8.0 (3.2)
Soil N	%	0.9 (0.4)	0.6 (0.4)
C:N	unitless	26.8 (3.1)	14.4 (1.8)
Soil Moisture	%	57.4 (15.0)	37.6 (7.2)
Soil pH	unitless	4.2 (0.3)	6.8 (0.5)
Microbial Biomass	μg CO_2-C hr^{-1} g^{-1} dry soil	9.0 (4.2)	8.7 (6.4)
Dominant Tree Species		Red oak (*Quercus rubra*), White pine (*Pinus strobus* L.), Red maple (*Acer rubrum* L.)	Red oak (*Quercus rubra*), Tulip poplar (*Liriodendron tulipifera* L.), Pignut hickory (*Carya glabra* Miller)
Soil Order		Spodosol, Inceptisol, Entisol	Alfisol
n		27	27

678

679 **Table 2** Model results from a linear regression model of cumulative mineralization rates
680 including laboratory treatments and microsite soil conditions from within HARV and SCBI sites.
681 Lab moisture was treated as a continuous variable to allow comparison with field soil moisture.
682 A second-order lab moisture term was included to capture the unimodal response where mesic
683 moisture conditions resulted in higher respiration rates. Standardized coefficients with their
684 standard error in parentheses are shown and were calculated by subtracting the mean and
685 dividing by 2 × standard deviation (SD) when there were categorical predictors, and one SD
686 when only continuous predictors were assessed. Unstandardized model results are presented in
687 supplemental information (Table S2).
688

	Both Sites (Full Model)	HARV (Full Model)	SCBI (Full Model)
Predictors	Standardized Estimates	Standardized Estimates	Standardized Estimates
(Intercept)	**3.91** (0.05)***	**4.08** (0.03)***	**4.22** (0.05)***
Site [HARV = 0]	**0.48** (0.09)***	na	na
Lab Moisture	**-0.31** (0.04)***	0.01 (0.02)	**-0.30** (0.03)**
Lab Moisture^2	0.03 (0.11)	**-0.07** (0.03)**	**0.09** (0.04)**
Field Soil Moisture	**0.14** (0.05)**	**0.08** (0.02)***	0.03 (0.03)
Soil pH	0.04 (0.05)	0.02 (0.02)	0.01 (0.03)
Soil Temperature	-0.06 (0.09)	0.00 (0.02)	-0.02 (0.03)
Lab Moisture × Field Soil Moisture	**0.25** (0.07)***	**-0.04** (0.02)*	0.00 (0.03)
Observations	162	81	81
R^2 / R^2 adjusted	52.7 / 50.5	36.7 / 31.5	62.8 / 59.8

*P < 0.05, **P < 0.01, ***P < 0.001; na: not applicable

689
690

691

692 **Figure legends**

693 **Fig. 1**. Soil moisture variation in sampling points from HARV (a) and SCBI (b) from Spring
694 2020. Values represent point measurements representative of the spatial range in moisture
695 regimes. Histogram represents the number of microsites, binned at 2.5% intervals with n = 27 per
696 site.

697

698 **Fig. 2.** Litter mineralization rates over 202 days. The upper panels (a-c) are shown here as the
699 mean carbon mineralization rate ($\mu g\ CO_2\text{-}C\ g^{-1}$ litter hr^{-1}) of each time point from litter
700 microcosms comprised of *Quercus rubra* litter and decomposer communities from HARV (solid
701 line) or SCBI (dashed line) sites. Laboratory treatments are presented from left to right of
702 increasing moisture conditions. Error bars are ±SD (n = 27). Bottom panels (d-f) represent
703 boxplots of cumulative mineralization over 202 days grouped by site. The median of each site is
704 within the 25th and 75th percentiles (interquartile range, IQR) shown as horizontal lines with
705 vertical lines extending to the first observation closest to but not exceeding 1.5*IQR. Each point
706 represents an observation.

707

708 **Fig. 3.** Cumulative mineralization (reported as mg CO_2-C mineralized g^{-1} litter) for unique
709 decomposer communities sourced from within the SCBI (a) and HARV (b) sites. Cumulative
710 values (for the 202-day incubations) are plotted against microsite soil moisture conditions (%
711 gravimetric soil moisture) from Spring 2020 and by the three laboratory moisture treatments that
712 were imposed on each community. Points (n=27 soil inocula per site) represent unique litter-soil
713 microcosms subjected to 35% of maximum water holding capacity (Dry: red points and quick

dashed line), 60% of maximum water holding capacity (Mesic: black points and long dashed line), and 100% of maximum water holding capacity (Wet: blue points and solid line). Note that the regression lines are not fit to the observations in a univariate manner. Instead, regression lines were calculated using unstandardized coefficients from the multiple regression models with non-log transformed cumulative respiration rates but otherwise are identical to models presented in Table 2. Note the different scales on the Y-axes.

Fig. 1

(a) Harvard Forest, MA (HARV)

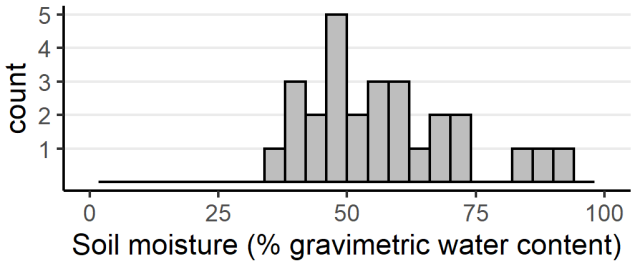

(b) Smithsonian Conservation Biological Institute, VA (SCBI)

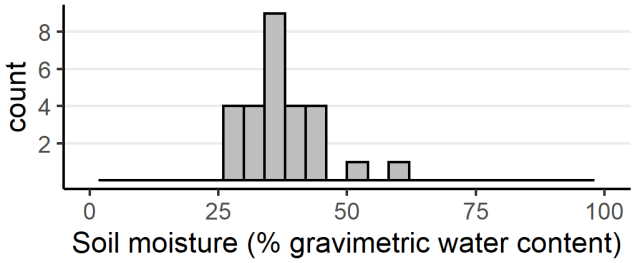

726 **Fig. 2**

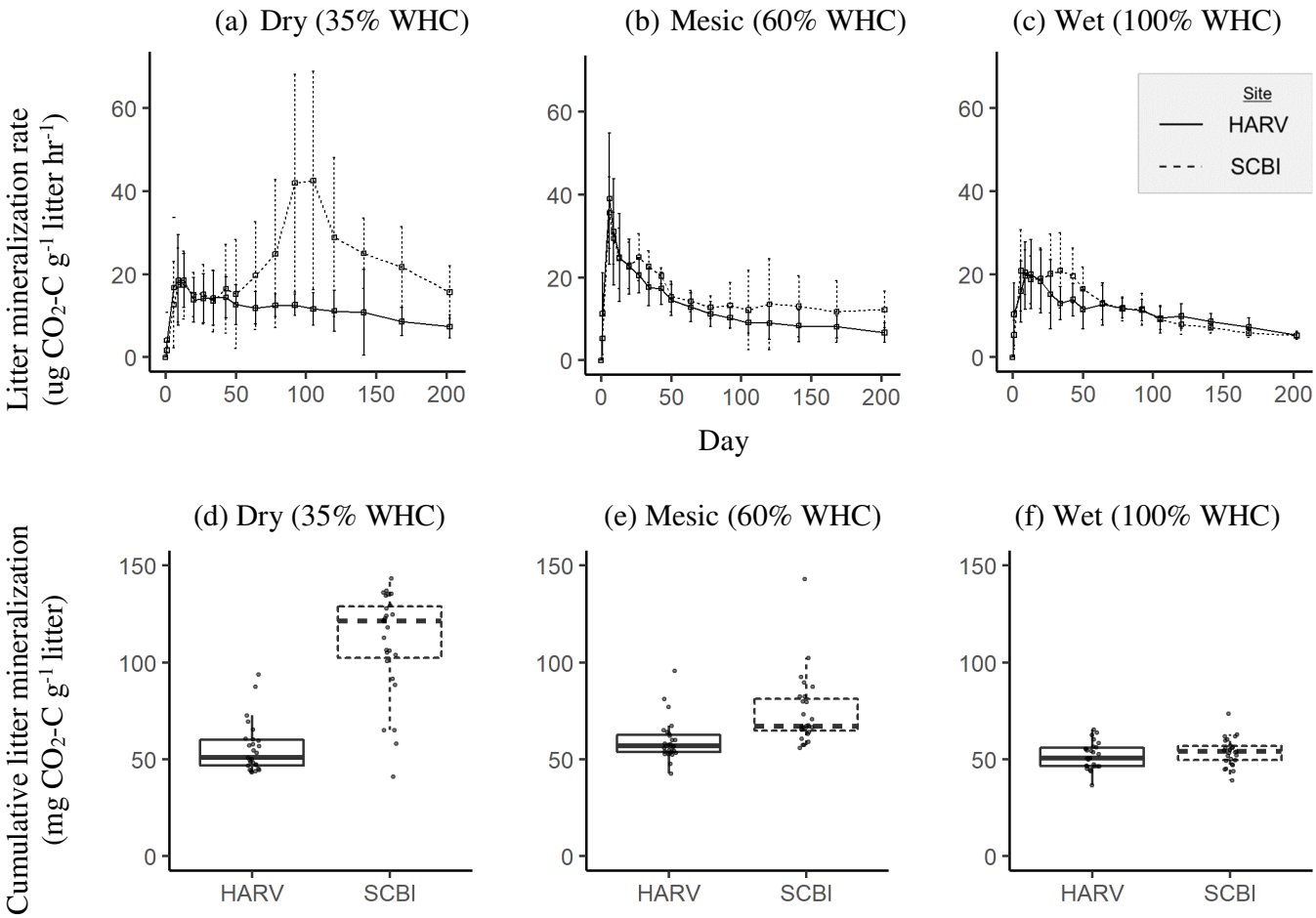
(a) Dry (35% WHC)
(b) Mesic (60% WHC)
(c) Wet (100% WHC)
Litter mineralization rate (ug CO2-C g-1 litter hr-1)
Site
HARV
SCBI
Day
(d) Dry (35% WHC)
(e) Mesic (60% WHC)
(f) Wet (100% WHC)
Cumulative litter mineralization (mg CO2-C g-1 litter)
HARV
SCBI

727

728 **Fig. 3**

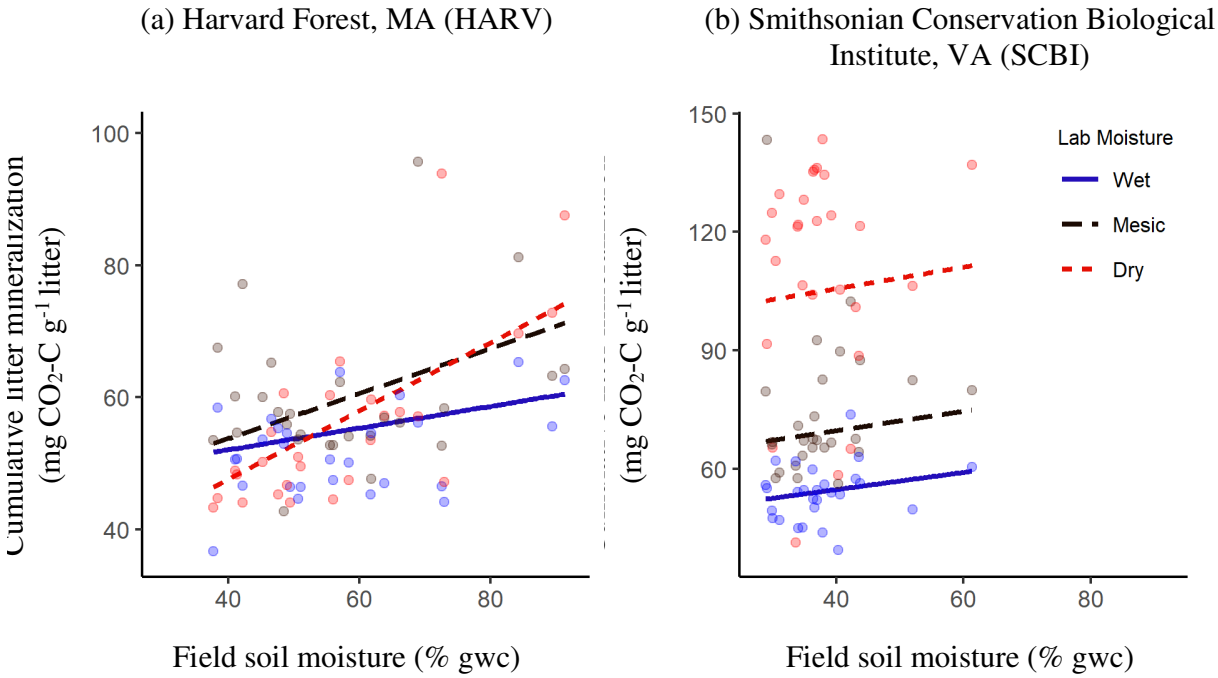
(a) Harvard Forest, MA (HARV)
(b) Smithsonian Conservation Biological Institute, VA (SCBI)
Cumulative litter mineralization (mg CO_2-C g^{-1} litter)
Field soil moisture (% gwc)
Field soil moisture (% gwc)
Lab Moisture
Wet
Mesic
Dry
100
80
60
40
150
120
90
60
40
60
80

729